Hydrogen production by steam reforming of dimethyl ether over Cu/ZnO/Al₂O₃ and H-ZSM-5 catalysts: An experimental and modeling study

Paria Amirshaghaghi [1], Ali Eliassi [2], Majid Taghizadeh [1,*]

[1] Chemical Engineering Department, Babol University of Technology, P.O. Box 484, 4714871167 Babol, Iran
[2] Chemical Technologies Research Department, Iranian Research Organization for Science and Technology (IROST), Tehran, Iran

Article Information	Abstract

Hydrogen was produced by steam reforming of dimethyl ether (DME) using a physical mixture of commercial HZSM-5 zeolite (for DME hydrolyzing) and Cu/ZnO/Al₂O₃ (for methanol steam reforming) as a catalyst in a fixed bed reactor. The experiments were performed at atmospheric pressure and in a temperature range from 270 to 310 °C. The effects of feed temperature and gas hourly space velocity (GHSV) between 2420 and 4615 h⁻¹ on DME conversion and H₂ and CO concentrations in the gas-phase products were investigated. In addition, the temperature changes along the catalyst bed were measured. The results showed that DME conversion increased with increasing temperature, and also, DME conversion decreased with increasing GHSV. Finally, a homogeneous one-dimensional model was used to model the reactor of hydrogen production by steam reforming of DME. The predicted temperature profile along the catalyst bed and conversion were compared with the experimental data. The model results and experimental data were found to be in good agreement.

1. Introduction

Sources of worldwide fossil fuels are rapidly reducing, whereas the energy consumption all over the world is increasing. It needs to have new and more alternative sources of energy. In addition, fossil fuels currently provide 80% of world energy [1]. Due to the high prices and environmental pollution of fossil fuels, there are many attempts to replace customary fossil fuels with clean sources of energy.

In recent years, the method of energy conversion in fuel cells has attracted much attention. The reason is that production of energy by fuel cell is clean and pollutants such as sulfur oxides, nitrogen oxides, carbon monoxide and dioxide will not produced by fuel cells and also the yield of fuel cells is very high. Hydrogen is the best fuel for fuel cells, which can be produced from reforming of natural gas, hydrocarbons (especially gasoline), alcohols and ethers. Using these chemicals to produce hydrogen has some advantages and disadvantages. Steam reforming of natural gas and gasoline needs high temperature (600 °C for natural

*Corresponding author: Tel: +98 11 32334204; fax: +98 11 32334201.
E-mail address: m_taghizadehfr@yahoo.com (M. Taghizadeh).

gas and more than 800 °C for gasoline) and a lot of energy consumption. However, steam reforming of methanol can be performed at lower temperatures (150–300 °C) [2]. On the other hand, methanol is more expensive than natural gas. In addition, one of the disadvantages of methanol is its biological poisonous behavior.

It should be mentioned that dimethyl ether and methanol might be directly produced from synthesis gas). While, DME is relatively inactive, non-corrosive, non-carcinogenic and virtually non-toxic and is recently proposed as a clean fuel due to producing extremely low NOx [3, 4]. Physical properties and therefore application and storage of dimethyl ether and LPG are similar. Hydrogen can be produced by dimethyl ether steam reforming and this method of hydrogen production is more profitable than steam reforming of methanol [5].

Steam reforming of dimethyl ether (DMESR) consists of two sequential endothermic reactions: First, hydrolysis of DME (DMEHYD) to methanol, second, steam reforming of methanol (MeOHSR) to carbon dioxide and hydrogen [6]:
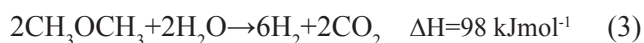
DMESR:
$$CH_3OCH_3 + 3H_2O \rightarrow 6H_2 + 2CO_2 \quad \Delta H = 123 \text{ kJmol}^{-1} \quad (1)$$

DMEHYD:
$$CH_3OCH_3 + H_2O \rightarrow 2CH_3OH \quad \Delta H = 25 \text{ kJmol}^{-1} \quad (2)$$

MeOHSR:
$$2CH_3OCH_3 + 2H_2O \rightarrow 6H_2 + 2CO_2 \quad \Delta H = 98 \text{ kJmol}^{-1} \quad (3)$$

Generally, the hydrolysis of dimethyl ether is occurring in the presence of catalytic acid such as alumina, zeolite, Ga_2O_3–TiO_2, WO_3–ZrO_2, while the methanol steam reforming occurs on Cu-, Pt-, Ru-, and Pb- catalysts [7–17].

In the literature, different models and simulations are presented about steam reforming of methane [18, 19] and methanol [20].

Previously, some kinetic models were proposed by researchers for DME hydrolysis [21–23]. For example Creaser et al. [21] have developed a global

kinetic model for autothermal reforming of dimethyl ether over a Pd-Zn/Al$_2$O$_3$ catalyst. In this work, hydrogen is produced by steam reforming of dimethyl ether and some different process parameters such as temperature and GHSV are changed and the effects of these parameters are investigated on DME conversion and hydrogen production. Also, a one-dimensional homogeneous model is used to model an adiabatic fixed-bed reactor for steam reforming of dimethyl ether. On the other hand, a kinetic model which was proposed by Patel and Pant [24] for steam reforming of methanol was used for DME steam reforming. The results showed that the axial temperature and conversion profiles in an adiabatic fixed-bed reactor for hydrogen production were well predicted by the proposed model. Also, some experiments were performed and the accuracy of the model was evaluated with the obtained experimental data.

2. Experiments

2.1. Materials

The used composite catalyst for steam reforming of DME was a physical mixture of commercial zeolite H-ZSM-5 (H-MFI90 of Süd-Chemie, AG-Germany) and Cu/ZnO/Al$_2$O$_3$ (MK-121 of Haldor Topsoe A/S). In order to prepare the composite catalyst, H-ZSM-5 and Cu/ZnO/Al$_2$O$_3$ powders were mixed in a ball mill in equal weight ratio and then the mixture was agitated for an hour. The obtained mixture was pressed under 10 bars and made into tablets by the press device. The tablets were crushed and sieved (16–25 mesh), until catalyst particles with an appropriate size for the reactor testing were achieved. Distilled water and dimethyl ether (GHC Gerling, Holz & Co., AG-Germany) with purity of 99.9% were used as reactants.

2.2 DME steam reforming

Steam reforming of DME was investigated in an adiabatic fixed bed reactor with an internal diameter of 1.27 cm. A schematic diagram of the experimental

apparatus is shown in Figure 1.

The reactor was filled with 15 g composite catalyst including equal weight ratio of acid catalyst and Cu catalyst based. All experiments were carried out at ambient pressure for 4 h in a fixed bed reactor (ID = 19 mm, L = 900 mm). Reactor feed was a mixture of DME and H_2O in a molar ratio of 1 to 3 at normal temperature and pressure (NTP).

2.3. The product analysis

When the temperature, pressure and feed and product flow rates were became constant (steady state conditions), the product was sent to an analyzer. For this purpose, the outlet reactor stream was cooled to room temperature and the remaining gas phase was directed to an online gas chromatograph instrument (Teif Gostar faraz Co., Iran). Two packed columns including (HYSEP Q, COSTOM, Iran, mesh 80–100)

for analyzing of DME and CH_3OH and (Molecular sieve 5A, mesh 60–80) for H_2 and CO analyzing were used. The gas chromatograph instrument was equipped with a thermal conductivity detector (TCD) and also with a flame ionization detector (FID). Finally, DME conversion was calculated by the following equation:

$$x_{DME}(\%) = \frac{F_{DME,in} - F_{DME,out}}{F_{DME,in}} \times 100 \qquad (4)$$

3. Modeling

3.1. The model assumptions

The fixed bed reactor model is based on the following assumptions:
- Ideal plug flow in the reactor is considered.
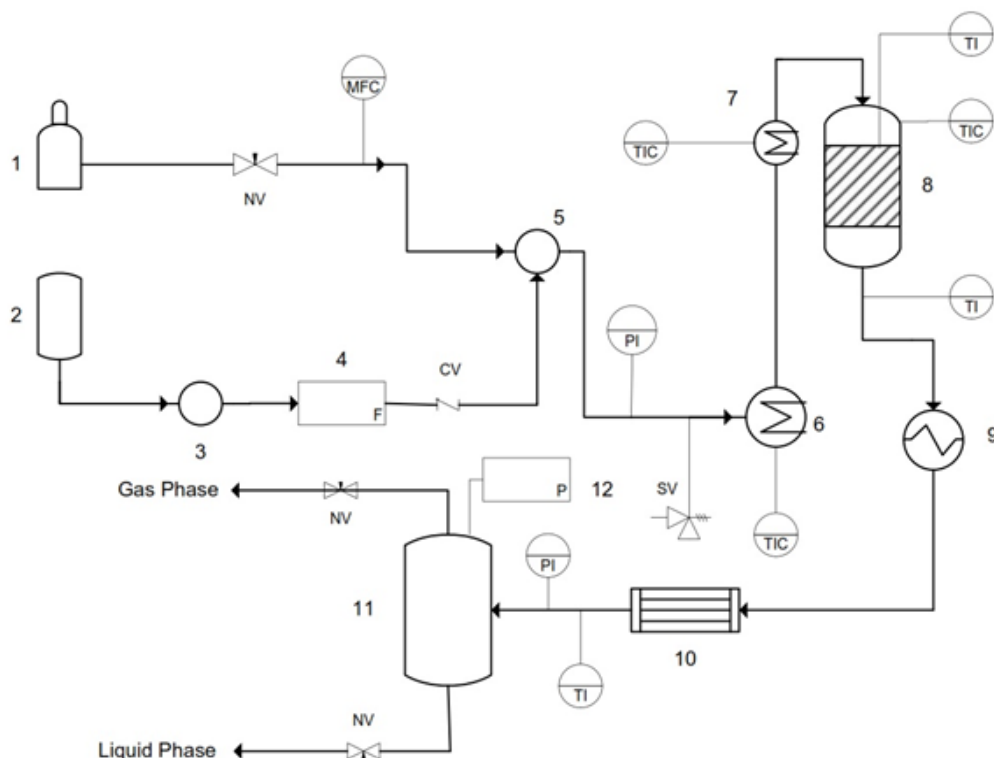- The system is in steady state conditions.

Figure 1. A schematic diagram of the experimental apparatus for steam reforming of DME: (1) DME cylinder, (2) water tank, (3) dosing pump, (4) Flow meter (5) Mixer, (6) evaporator, (7) preheater, (8) adiabatic fixed bed reactor, (9) air cooler, (10) condenser, (11) liquid-gas separator, (12) Back pressure regulator.

• The reactor is considered adiabatic.
• The pressure drop across the reactor is negligible.
• The temperature gradient in the radial direction is neglected.
• Concentration changes in the radial direction are neglected and it is assumed that there are not any convection and diffusion streams in the radius direction.
• The diffusion of materials into the catalysts is neglected.

3.2. Equations

One dimensional heterogeneous model and simulation of the fixed bed reactor are selected. The mass and energy balance equations for the gas phase can be written as follows:

- Energy balance of the gas phase inside the reactor:

$$u\rho c_p \frac{dT^b}{dz} = \sum r_M \left(T^b, C_i^b\right)\left(-\Delta H_r\right)\rho_B \qquad (5)$$

- Mass balance of the components in the reactor:

$$-u \frac{dC_i^b}{dz} = \sum v_i r_M \left(T^b, C_i^b\right)\rho_B \qquad (6)$$

Parameters for DME hydrolysis presented by Creaser et al. [21] and the reaction rate and kinetic parameters proposed by Patel and Pant [24] for modeling and simulation of methanol steam reforming were used in this work. The equations used in this study are presented as follows:

$$r_{(DME\,hyd)} = \frac{k_{m2} \exp\left(\frac{E_{A2}}{R}\left(\frac{1}{T_m} - \frac{1}{T}\right)\right) y_{DME}\, y_{H_2O}}{\left(1 + K_{m2} \exp\left(\frac{\Delta H_{ads}}{R}\left(\frac{1}{T_m} - \frac{1}{T}\right)\right) y_{H_2O}\right)^2} \qquad (7)$$

$$r_{SRM} = \frac{k_r K_{O(1)} K_{CH_2O(1)} \left(\dfrac{P_{CH_3OH}P_{H_2O}}{P_{H_2}^2}\right)\left(1 - \dfrac{P_{H_2}^3 P_{CO_2}}{K_r^* P_{CH_3OH} P_{H_2O}}\right)}{\left(\begin{array}{l} 1 + \dfrac{K_{CH_3O(1)}P_{CH_3OH}}{P_{H_2}^{1/2}} + \dfrac{K_{OH(1)}P_{H_2O}}{P_{H_2}^{1/2}} + \dfrac{K_{O(1)}P_{H_2O}}{P_{H_2}} \\[2ex] + \dfrac{K_{CH_2O(1)}P_{CH_3OH}}{P_{H_2}} + K_{HCOO(1)}P_{H_2}^{1/2}P_{CO_2} \end{array}\right)^2} \qquad (8)$$

The kinetic parameters of the equations (7) and (8) are reported in Table 1.

Table 1. Kinetic parameters of equations (7) and (8) [22].

k_r (J mol^{-1} K^{-1})	9.14×10^9
$K_{O(1)}$ (J mol^{-1} K^{-1})	-37.2
$K_{CH_2O(1)}$ (J mol^{-1} K^{-1})	-41.5
K_r^* (J mol^{-1} K^{-1})	87.6
$K_{CH_3O(1)}$ (J mol^{-1} K^{-1})	-32.3
$K_{OH(1)}$ (J mol^{-1} K^{-1})	-46.8
$K_{HCOO(1)}$ (J mol^{-1} K^{-1})	162.3
k_{m2} (mol kg^{-1} s^{-1})	59.00
E_{A2} (kJ mol^{-1})	173.9
K_{m2} (mol kg^{-1}s^{-1})	3.871
ΔH_{ads} (kJ mol^{-1})	-31.71
T_m (K)	300

3.3. Numerical solution of the equations

The energy equation for the reactor temperature and the mass equations for each component should be solved simultaneously. The boundary condition equations are:

$$C_i^b = C_{i,0}^b \quad \text{at} \quad z = 0 \qquad (9)$$
$$T^b = T_0^b \quad \text{at} \quad z = 0 \qquad (10)$$

MATLAB 7.8.0.347 has been used to solve these equations. For the integration of the equations of mass and energy balances in the reactor, the fourth order Runge-Kutta method was used.

4. Results and Discussion

The model results and the obtained experimental data are shown in Figures 1 to 9.

4.1. Temperature changes in the catalyst bed

Figures 2–4 show the temperature variations of the

catalyst bed at three different feed temperatures and two different gas hourly space velocities. According to the results, the temperature gradient is not fixed along the reactor catalyst bed. So that, the temperature gradient in the reactor inlet is high, and gradually the temperature changes are decreased. This phenomenon can be explained by endothermic behavior of the DME steam reforming. At the beginning of the reaction, the reaction rate is high and the rate of temperature decreasing is high. When the reaction proceeds, the reaction rate is decreased, so that the temperature gradient is decreased, too. By increasing GHSVs or decreasing the residence time, the rate of temperature decreasing is increased, which is obvious.
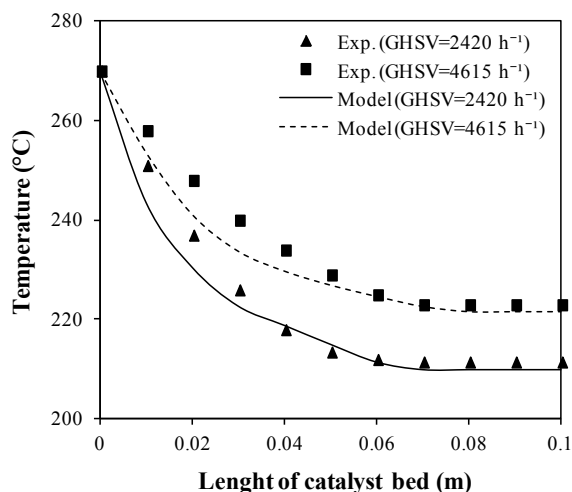

Figure 2. Catalyst bed temperature versus reactor length at two different GHSVs. Feed conditions: T = 270 °C, P = 1 atm.
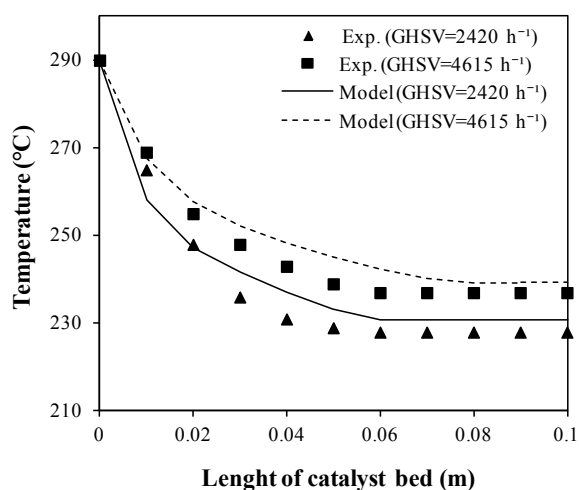

Figure 3. Catalyst bed temperature versus reactor length at two different GHSVs. Feed conditions: T = 290 °C, P = 1 atm.

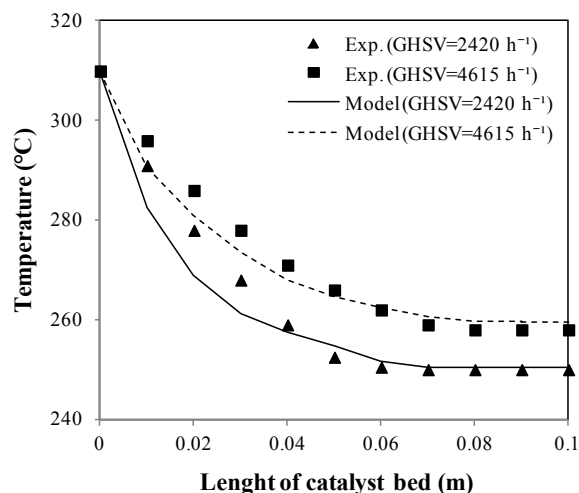**Figure 4. Catalyst bed temperature versus reactor length at two different GHSVs. Feed conditions: T = 310 °C, P = 1 atm.**

4.2. The influence of feed temperature and GHSV on the conversion of dimethyl ether

In Figures 5-7 DME conversions versus length of catalyst bed have been shown. According to these figures, the DME conversion increases with increasing temperature. In addition, with increasing GHSV (2420–4615 h^{-1}), the DME conversion is reduced which is due to the residence time decreasing.

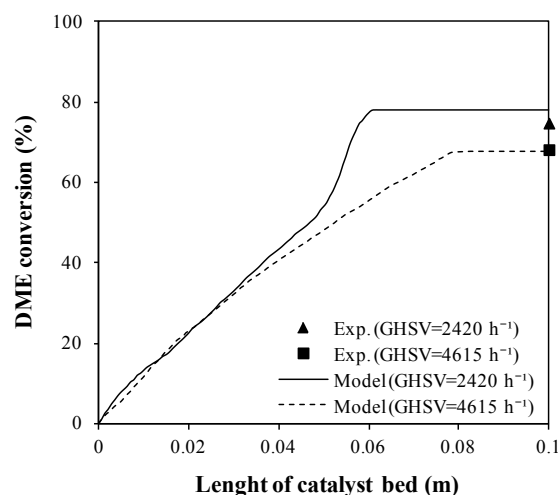**Figuur 5. DME conversion versus length of catalyst bed at two different GHSVs. Feed conditions: T = 270 °C, P = 1 atm.**

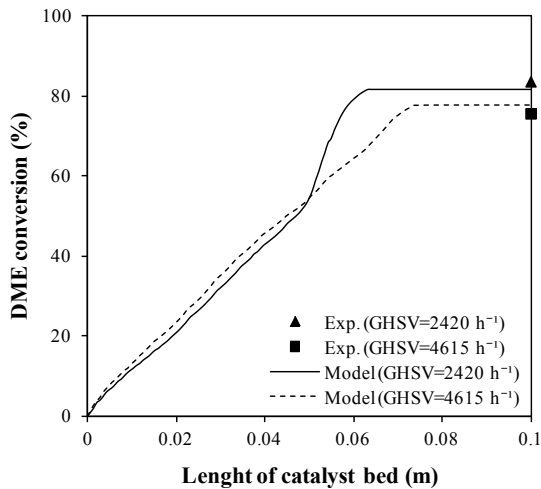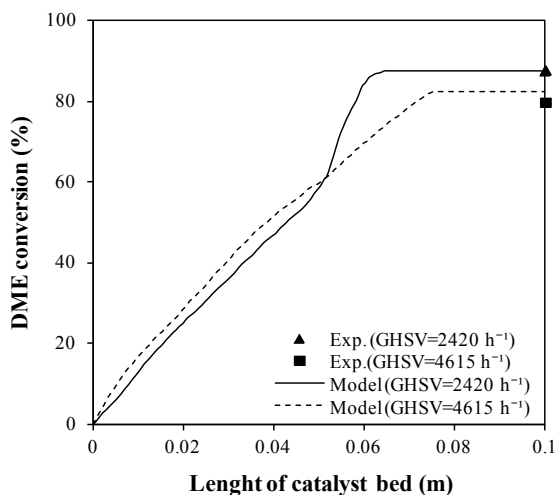**Figure 6. DME conversion versus length of catalyst bed at two different GHSVs. Feed conditions: T = 290 °C, P = 1 atm.**

Figure 7. DME conversion versus length of catalyst bed at two different GHSVs. Feed conditions: T = 310 °C, P = 1 atm.

The conversion of DME at different feed temperatures and GHSVs are measured and are shown in Figure 8. The results show that, with increasing the temperature, the conversion of DME is increased and with increasing GHSV, the DME conversion decreases.

4. 3. The influence of temperature and GHSV on H_2 concentration

The concentration of H_2 at different feed temperatures and GHSVs are measured and shown in Figure 9. It can be observed that when GHSV is 2420 h⁻¹, the maximum volume concentration of H_2 is obtained at
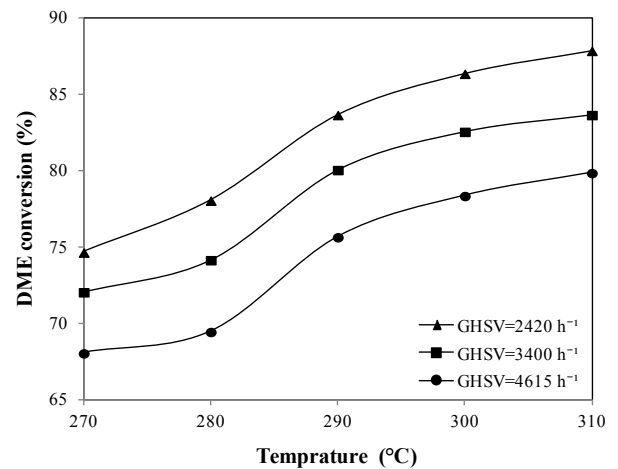

Figure 8. The measured or experimental DME conversion versus feed temperature at different GHSVs.

290 °C but when GHSV is 4615 h⁻¹, the maximum concentration of H_2 is obtained at 310 °C. In general, the obtained results show that by increasing the residence time and temperature selectivity respect to hydrogen production is better than the reverse conditions. On the other hand, at higher temperature (for example 310 °C) hydrogen concentration decreased or selectivity respect to hydrogen production is decreased.
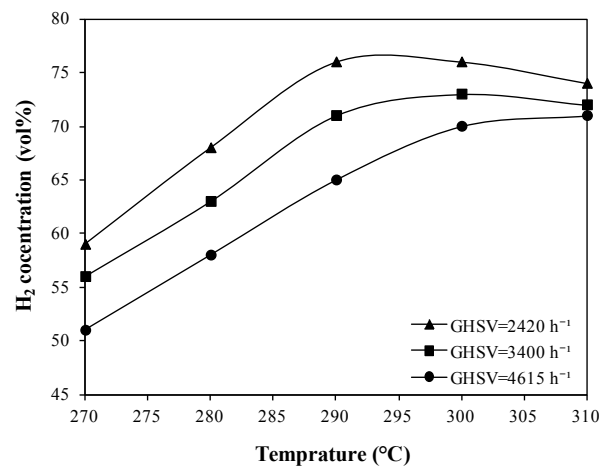

Figure 9. The measured or experimental H_2 concentration versus feed temperature at different GHSVs.

Figure 10 shows the measured CO and H_2 concentrations in the products versus temperature at a fixed value of GHSV. According to this figure CO concentration is nearly constant against the

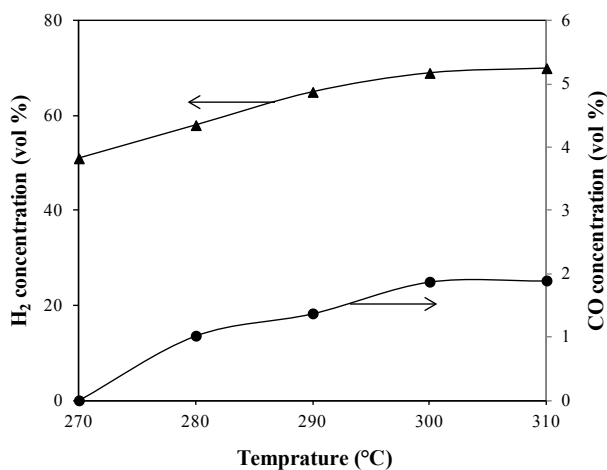temperature changes, but H_2 concentration clearly increases against temperature.

Figure 10. The measured or experimental H_2 and CO volume concentrations versus feed temperature at GHSV = 2420 h⁻¹ and P = 1 atm.

4.5. Relative deviation calculations

For comparing the simulation results with the experimental data, the simulated and measured values accompanied with the relative deviations in percentage terms are reported in Table 2.

5. Conclusions

Steam reforming of dimethyl ether was studied in this work and some experimental measurements were done using a commercial catalyst at different temperatures and GHSVs. Also, a one-dimensional model was developed to simulate the adiabatic fixed bed reactor for steam reforming of DME. The temperature and DME conversions along the catalyst bed in an adiabatic fixed bed reactor were predicted by the model and compared with the experimental results. Furthermore, the influences of feed temperature and GHSVs (2420–4615 h⁻¹) on DME conversions were studied. The results showed that the DME conversion increases with increasing temperature, and also, the DME conversion generally decreases with increasing GHSV. The temperature change along the catalyst bed showed that temperature gradient is high at the inlet portion of the reactor and it is gradually reduced along the catalyst bed. On the other hand the concentration of hydrogen in the gas product is increased by temperature increasing up to 300 °C and GHSV decreasing. But, at the higher temperature, e.g. 310 °C, the hydrogen concentration was decreased, probably due to the decrease in selectivity with

Table 2. Comparison of the simulation results and experimental data at P = 1 atm.

NO.	T (°C)	GHSV (h⁻¹)	Experimental DME conversion (%)	Model DME conversion (%)	Relative deviation* (%)
1	270	2420	74.7	78.01	−4.43
2	280	2420	78.1	78.68	−0.75
3	290	2420	83.7	81.8	2.27
4	300	2420	86.4	83.9	2.9
5	310	2420	87.9	87.42	0.55
6	270	3400	72.1	68.42	5.1
7	280	3400	74.2	77.7	−4.72
8	290	3400	80.1	79.76	0.43
9	300	3400	82.6	81.32	1.55
10	310	3400	83.7	87.06	−4.011
11	270	4615	68.1	67.71	0.57
12	280	4615	69.5	73.74	−6.10
13	290	4615	75.7	77.77	−2.73
14	300	4615	78.4	81	−3.32
15	310	4615	79.9	78.56	1.68

* $RD\% = 100 \times (x_{exp} - x_{cal})/x_{exp}$

respect to hydrogen production. Finally, there is a good consistency between the experimental data and the results of the proposed model.

6. Acknowledgment

NOMENCLATURE

C	Concentration in fluid phase, kmol m^{-3}
c_p	Specific heat of fluid, kJ kg^{-1} K^{-1}
x	Conversion
F	Molar flow rate of DME, mol s^{-1}
ΔH	Heat of reaction, kJ kg mol^{-1}
K	Thermodynamic equilibrium constant, J mol^{-1} K^{-1}
P	Pressure, atm
r	Reaction rate, mol m^{-2} s^{-1}
T	Temperature, K
u	Superficial velocity, m h^{-1}
z	Reactor longitude coordinate, m
Y	Mole fraction
k	Reaction rate constant, mol kg^{-1} s^{-1}
E	Activation energy, kJ mol^{-1}

Greek letters

v	Stoichiometry coefficient
ρ	Gas phase density, kg m^{-3}
ρ_B	Catalyst bed density, kg m^{-3}

Subscripts

i	ith component
1	index for methanol reforming reaction
2	index for DME hydrolyze reaction
M	Methanol
Ads	Adsorption
0	Inlet condition
s	Surface conditions
m	mean
DME$_{hyd}$	DME hydrolysis

Superscripts

b	bulk condition

7. References

[1] Marban G., Valdes-Solis T., "Towards the hydrogen economy?", Int. J. Hyd. Eng., 2007, 32(12): 1625.

[2] Palo D. R., "Methanol steam reforming for hydrogen production", Chem. Rev., 2007, 107: 3992.

[3] Kawabata T., Matsuoka H., Shishido T., Li D., Tian Y., Sano T., Takehira K., "Steam reforming of dimethyl ether over ZSM-5 coupled with Cu/ZnO/Al$_2$O$_3$ catalyst prepared by homogeneous precipitation", Appl. Catal. A: Gen., 2006, 308: 82.

[4] Topp-Jorgensen J., "Reacting crystalline aluminosilicate with nitrogen containing base, then desorption aftertreatment" U.S. Patent No. 4536485, 1985.

[5] Dybkjir I., Hansen J.B., "Large scale production of alternative synthetic fuels from natural gas", Stud. Surf. Sci. Catal., 1997, 107: 99.

[6] Solymosi F, Barthos R, Kecskemeti A., "The decomposition and steam reforming of dimethyl ether supported Mo2C catalysts", Appl. Catal. A, 2008, 350(1): 30.

[7] Badmaeva S.D., Snytnikov P.V., "Hydrogen production from dimethyl ether and bioethanol for fuel cell applications", Int. J. Hydrogen Energy, 2008, 33(12): 3026.

[8] Mathew T., Yamada Y., Ueda A., Shioyama H.,

Kobayashi T., Gopinath C.S., "Effect of support on the activity of Ga2O3 species for steam reforming of dimethyl ether", Appl. Catal. A., 2006, 300(1): 58.

[9] Matsumoto T., Nishiguchi T., Kanai H., Utani K., Matsumura Y., Imamura S., "Steam reforming of dimethyl ether over H-mordenite-Cu/CeO$_2$ catalysts", Appl. Catal. A., 2004, 276(1): 267.

[10] Nishiguchi T., Oka K., Matsumoto T., Kanai H., Utani K., Imamura S., "Durability of WO3/ZrO$_2$-CuO/CeO$_2$ catalysts for steam reforming of dimethyl ether", Appl. Catal. A., 2006, 301(1): 66.

[11] Wang X., Pan X., Lin R., Kou S., Zou W., Ma J.X., "Steam reforming of dimethyl ether over CueNi/g Al$_2$O$_3$ bi-functional catalyst prepared by deposition precipitation method", Int. J. Hydrogen Energy, 2010, 35(9): 4060.

[12] Takeishi K., Suzuki H., "Steam reforming of dimethyl ether", Appl. Catal. A., 2004, 260(1): 111.

[13] Galvita V.V., Semin G.L., Belyaev V.D., Yurieva T.M., Sobyanin V.A., "Production of hydrogen from dimethyl ether", Appl. Catal. A., 2001, 216(1): 85.

[14] Semelsberger T.A., Ott K.C., Borup R.L., Greene H.L., "Generating hydrogen-rich fuel-cell feeds from dimethyl ether (DME) using Cu/Zn supported on various solid-acid substrates", Appl. Catal. A., 2006, 309(2): 210.

[15] Fukunaga T., Ryumon N., Shimazu S., "The influence of metals and acidic oxide species on the reforming of dimethyl ether (DME)", Appl. Catal. A., 2008, 348(2): 193.

[16] Yamada Y., Mathew T., Ueda A., Shioyama H., Kobayashi T., "A novel DME steam-reforming catalyst designed with fact database on-demand", Appl. Surf. Sci., 2006, 252(7): 2593.

[17] McHugh K., "Hydrogen Production Methods", MPR Associates Inc., 2005, p. 41.

[18] Avcm A. K., Trimm D.L., İlsen Önsan Z., "Heterogeneous reactor modeling for simulation of catalytic oxidation and steam reforming of methane", Chem. Eng. Sci., 2001(56): 641.

[19] Lee D.K., Baek I.H., Yoon W.L., "Modeling and simulation for the methane steam reforming enhanced by in situ CO$_2$ removal utilizing the CaO carbonation for H$_2$ production", Chem. Eng. Sci., 2004, 59: 93.

[20] Halabi M.H., de Croon J.M., Van der Schaaf J., Cobden P.D., Schouten J.C., Modeling and analysis of auto thermal reforming of methane to hydrogen in a fixed bed reformer", Chem. Eng. J., 2008, 137: 568.

[21] Creaser D., Nilsson M., Pettersson L.J., Dawody J., "Kinetic modeling of auto thermal reforming of dimethyl ether", Ind. Eng. Chem. Res., 2010, 49: 9712.

[22] Feng D., Wang Y., Wang D., Wang J., "Steam reforming of dimethyl ether over CuO–ZnO–Al$_2$O$_3$–ZrO$_2$ + ZSM-5: A kinetic study", Chem. Eng. J., 2009, 146: 477.

[23] Namuangruk S., Faungnawakij K., "Experimental and theoretical investigations on the hydrolysis of dimethyl ether to methanol over H-ZSM-5", Nanotechnology joint symposium with nano Korea, 2010.

[24] Patel S., Pant K.K., "Experimental study and mechanistic kinetic modeling for selective production of hydrogen via catalytic steam reforming of methanol", Chem. Eng. Sci., 2007, 62: 2425.